Nano World Journal

https://doi.org/10.17756/nwj.2023-s3-159

Research Article

Open Access

Investigation on the Mechanical Properties and Strengthening Mechanisms of AA5052 by Cryogenic Rolling

Vijay Ramarao Khawale[1], Venugopal Muniraju Maragondanahalli[2], Satishkumar Palanisamy[3*], Pallavi Singh[4], Hashim Mohammed Shajahan[5], Sudarshan Thalaguru Appaswamy[6] and Hariprasad Krishnasamy[7]

[1]Department of Mechanical Engineering, Yeshwantrao Chavan College of Engineering, Nagpur, India
[2]Department of Aeronautical Engineering, Nitte Meenakshi Institute of Technology, Bangalore, India
[3]Department of Mechanical Engineering, Rathinam Technical Campus, Coimbatore, Tamil Nadu, India
[4]Department of Biotechnology, Graphic Era Deemed to be University, Dehradun, Uttarakhand, India
[5]Scholar of Natural Sciences and Engineering, National Institute of Advanced Studies, IISc Campus, Bangalore, India
[6]Department of Mechanical Engineering, New Horizon College of Engineering, Bangalore, India
[7]Department of Science and Humanities, Rathinam Technical Campus, Coimbatore, Tamil Nadu, India

[*]Correspondence to:
Satishkumar Palanisamy
Department of Mechanical Engineering,
Rathinam Technical Campus,
Coimbatore, Tamil Nadu, India.
E-mail: sp.sathishkumar10@gmail.com

Received: July 31, 2023
Accepted: November 01, 2023
Published: November 03, 2023

Citation: Khawale VR, Maragondanahalli VM, Palanisamy S, Singh P, Shajahan HM, et al. 2023. Investigation on the Mechanical Properties and Strengthening Mechanisms of AA5052 by Cryogenic Rolling. *Nano World J* 9(S3): S896-S901.

Published by United Scientific Group

Abstract

Research was done on the mechanisms of strengthening underlying the mechanical characteristics of AA5052, as well as the effects of room-temperature rolling (RTR) and cryogenic rolling (CR). The results show that cryo-processing AA5052 significantly reduces the size of second-stage and sub-grain particles in addition to increasing dislocation density. When compared to RTR, CR processing considerably improves the ultimate tensile strength (UTS), yield strength (YS), and elongation (El) of AA5052. This is because of the synergistic effects of a finer grain structure and increased strength from dislocations.

Keywords

AA5052, Mechanical properties, Cryogenic rolling, Mechanical behaviour, Room-temperature rolling

Introduction

Due to their excellent formability, ductility and corrosion resistance, aluminum alloys containing Mg and Fe as the principal alloying components have found widespread use [1]. Aluminum alloys are in high demand because of their strength and the rapid growth of the automotive and aerospace industries. It is widely acknowledged that metallic materials can gain significantly from the development of a nanocrystalline structure in terms of both strength and ductility [2].

In recent years, CR has gained traction as a potentially game-changing method for the industrial production of nanocrystalline or ultrafine-grained metallic materials. The author has performed extensive research [3] on the mechanical characteristics of metals during CR. Author [4] reported that cryo-rolled high-purity copper, which contains nano-crystalline or ultrafine grains (< 300 nm), had remarkable mechanical properties. Increases of 23% for YS, 20% for UTS, and 92% for EL were seen when RTR-treated copper was compared to untreated copper [5]. As a result, nanocrystalline grains form and the dislocation density rises. Tensile characteristics of AA6082 were studied, and the author found that the rolling temperature made a difference.

Higher YS and UTS values were found for cryo-rolled AA6082 compared to equal thickness reductions in room-temperature rolled AA6082 [6]. When the deformation temperature is decreased and deformation ratio is increased,

the course second-phase of AA2219 fragments more quickly, as discovered by author [7]. This procedure significantly enhances the alloy's mechanical characteristics. According to the previously cited author's research [8], CR CP-Ti at a strain of 0.1 greatly raised the frequency of twin nucleation. Twins' wall thickness decreased from 1.2 m to 0.7 m when exposed to strains as high as 0.36% [9]. Many smaller sub-grains, with sizes ranging from 100 to 200 nm, were created at stresses greater than 0.9. If strain is increased to its maximum of 2.68, the grain size or sub grain lowers to 82 nm [10]. According to the author's detailed description [11], CR can greatly enhance the mechanical characteristics of Cu-3Ag-xZr, Titanium-6Al-4V, and Fe-25Cr-20Ni.

As was previously indicated [12], CR yields materials that are robust and ductile. High displacement densities can be attained because of the effective suppression of dynamic recovery at ultra-low temperatures, which is advantageous for both grain refinement and the improvement of mechanical characteristics of metallic materials. CR was used to improve AA5052's mechanical properties in this investigation. The reinforcing techniques that led to the enhanced mechanical properties were also investigated.

Experimentation

The components present in the hot-rolled AA5052 sheet used in this analysis are detailed in table 1. After being hot rolled, the AA5052 sheets were heated at 20 °C/min for six hours, until they reached 600 °C, and then immediately quenched in water. Pieces 160 mm × 60 mm in size were then sliced from sheets of AA5052 that had been solution treated (ST). The impact of strengthening methods on the mechanical characteristics of AA5052 ST sheets were studied by CR. This meant that the rolling experiment had to be carried out in phases. A preliminary immersion period of about 20 min is recommended for the sheet sample. To achieve the desired degree of distortion, the experiment was repeated using a fresh sheet sample iced in liquid nitrogen for 10 min. The thickness of these sheets was reduced by 30, 60, and 90% CR (CR 30, 60 and 90). After applying the same rolling at room temperature method to the remaining ST sheets, the thickness of the material decreased (RTR 30, 60, 90).

Sheets were rolled to 22 mm in width and 5 mm in thickness along the rolling direction, and the resulting pieces were machine-cut into dog-bone tensile samples. The rolled sheets and tensile specimens were of the same thickness [13, 14]. The UTM was used to do tensile testing at a speed of 1 mm/min. For each therapy, tests were conducted three times.

Results and Discussion

Figure 1 displays the engineering strain - stress curvatures that resulted from applying RTR and CR to ST specimens. As shown in figure 2, mechanical properties can be determined by calculating tensile curvatures for varying degrees of distortion. The ST specimen had an EL of 47.1%, a UTS of (127 ± 1) MPa and YS of (61 ± 2) MPa. YS and UTS were both higher for the 30% RTR specimen than for the ST sample ((138 ± 2) and (149 ± 1) MPa, respectively). Despite this, the (16.3 ± 0.2%) El was lower than the ST sample. While raising the rolling reduction from 30% to 90% dropped the El from 16.1 ± 0.3% to 13.8 ± 0.3%, the YS and UTS significantly rose from 138 ± 3% and 149 ± 3% to 173 ± 11% and 190 ± 2% MPa, respectively. This study shows that RTR processing reduces ductility while increasing strength.

Table 1: AA5052 (wt. %) chemical composition.

Material	Mg	Cr	Cu	Fe	Mn	Si	Zn	Al
Wt. %	2.2 - 2.8	0.15 - 0.35	0.1	0.4	0.1	0.25	0.1	Bal

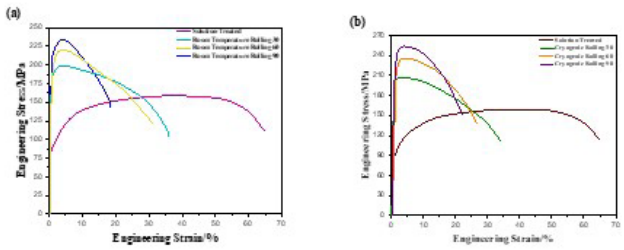

Figure 1: Engineering stress-strain curvature.

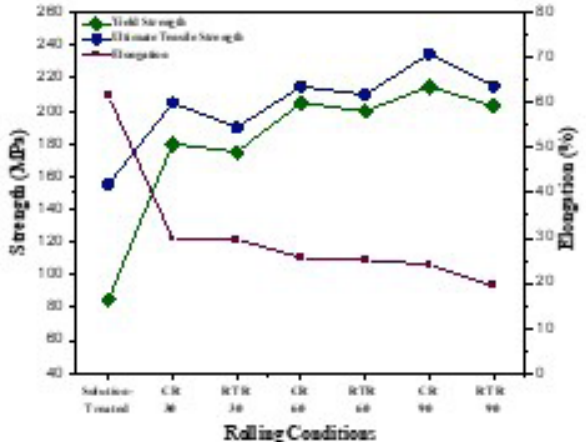

Figure 2: Variations in mechanical properties of the specimen under different rolling conditions.

UTS, YS, and El of the CR samples were (207 ± 0.3MPa), (182 ± 3 MPa), and (31.8 ± 0.3%), after being reduced in size by 30% via rolling. When the rolling reduction was increased from 30 to 90%, the EL dropped from 31.8 ± 0.2% to 3.1 ± 0.2%, and the YS and UTS jumped from 182 ± 4 and 207 ± 5 MPa, respectively, to 217 ± 3 MPa, a significant increase. This demonstrates that the CR technique has little to no effect on ductility, allowing for a larger rise in YS and UTS. Comparing the UTS, YS, and EL of a CR sample with the same rolling decrease as a RTR sample yielded some interesting findings. Once the rolling reduction reached thirty %, the UTS, YS, and El of the CR sample were 9.7%, 16.2%, and 9.5% greater than those of the RTR specimen. CR increased the specimen's YS and UTS at 90% rolling reduction by 8.1% and 9.7%, respectively, while the RTR specimen's EL increased by a far more modest 6.8%. Since CR improves AA5052's strength and ductility simultaneously, it is preferable to RTR for enhancing the material's mechanical properties [15].

Misorientation angles between 2 and 15° are shown distributed across different rolling conditions in figure 3. Figure 3a and 3b show that the average misorientation angle for the CR 30 samples is (5.012 ± 0.006)°, while the mean misorientation angle for the RTR 30 specimens is (5.196 ± 0.006)°. Figure 3c and 3d show that as the rolling decrease was raised from 30% to 90%, the average misorientation angle rose from (6.099 ± 0.015)° to (9.852 ± 0.015)°. Samples treated with CR have a slightly larger misorientation angle on average than RTR samples subjected to the same amount of rolling reduction processing.

The outcomes of rolling samples treated with a solution are depicted in figure 4. Higher levels of rolling reduction were found to result in smaller grain sizes [16, 17]. The cryo sample's mean grain size was significantly smaller than the RTR sample's when the two samples had the same rolling reduction [18].

The UTS and YS of the treated samples by rolling at ambient temperature and rolling at cryogenic temperatures were both significantly greater than those of the ST specimen. Strengthening processes like precipitation, dislocations, and grain refining [18]. As rolling reduction was increased, the UTS and YS of the CR specimen rose while the El of the RTR specimen fell. When compared to RTR specimens that had the same rolling reduction, cryotreated samples exhibited considerably higher UTS, YS, and EL. The findings show that CR processing enhances AA5052's YS, UTS, and El in comparison to RTR processing [19]. Since sub-grain size can be reduced through CR processing, the resulting displacement shape can contain several displacement causes, increasing total capacity [20, 21]. This is why CR specimens have such a high EL.

The strengthening influence of the CR method on the mechanical features of AA5052 was statistically analysed by computing the strengthening increments $(\Delta\sigma_Y = \sigma_{YCR} - \sigma_{YRTR})$ of the variance in the YS between the RTR and CR process (Figure 5). Alloys of varied rolling reductions had $\Delta\sigma_Y$ values higher than 10 MPa. CR and RTR resulted in different contributions to strength from dislocations, precipitation, and grain refinement. This research characterises the incremental value of YS $\Delta\sigma_Y$ [22].

$$\Delta\sigma_Y = \Delta\sigma_p + \Delta\sigma_{dis} + \Delta\sigma_{gb} \quad (1)$$

Whereas $\Delta\sigma_{gb}(\Delta\sigma_{dis} = \sigma_{disCR} - \sigma_{disRTR})$, and $\Delta\sigma_p(\Delta\sigma_p = \sigma_{PCR} - \sigma_{PRTR})$, $\Delta\sigma_{dis}(\Delta\sigma_{dis} = \sigma_{disCR} - \sigma_{disRTR})$ YS increases between RTR and CR situations by three distinct mechanisms: dislocation, precipitation, and grain refinement strengthening.

Orowan [23] shown that a dislocation can create a loop around particles anywhere it slides, even if it bypasses them without shearing them, if it is moving down its glide plane. The Orowan by-pass modelling suggested in [24] can be used to assess the effect of incoherent particle (σp) to the YS (σγ).

$$\sigma_p = \frac{0.84MGb}{2\pi\lambda(1-\nu)^{0.5}} \ln\frac{r}{b} \quad (2)$$

$$\lambda = r\left(\frac{2\pi}{3f}\right)^{\frac{1}{2}} \quad (3)$$

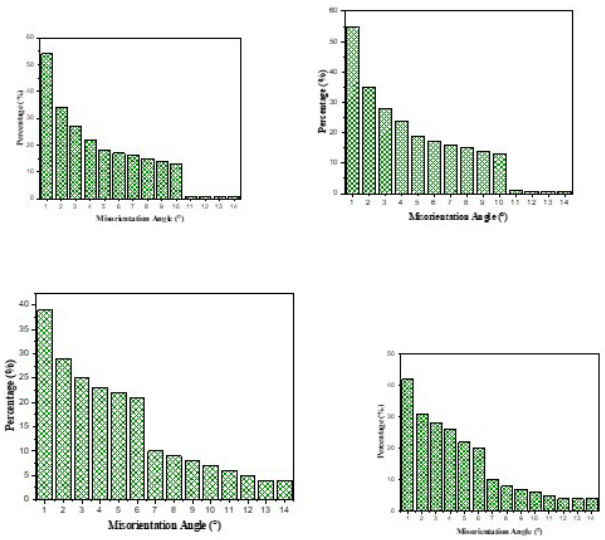

Figure 3: Distribution of misorientation angles: **(a)** CR 30, **(b)** RTR 30, **(c)** CR 90, and **(d)** RTR 90.

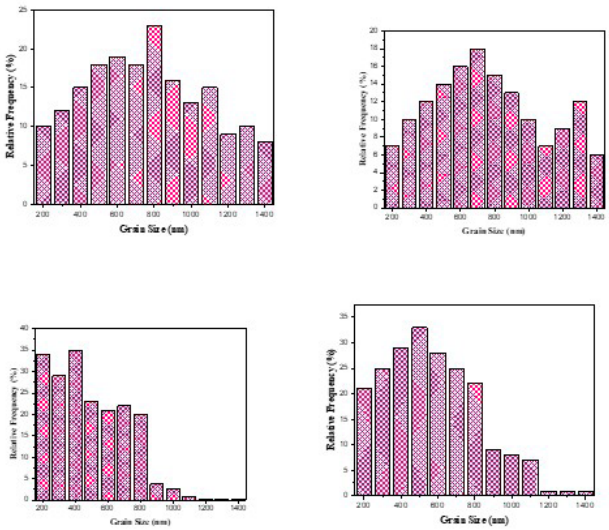

Figure 4: Grain size distribution of a ST specimen rolled in various conditions: **(a)** CR 30, **(b)** RTR 30, **(c)** CR 90, and **(d)** RTR 90.

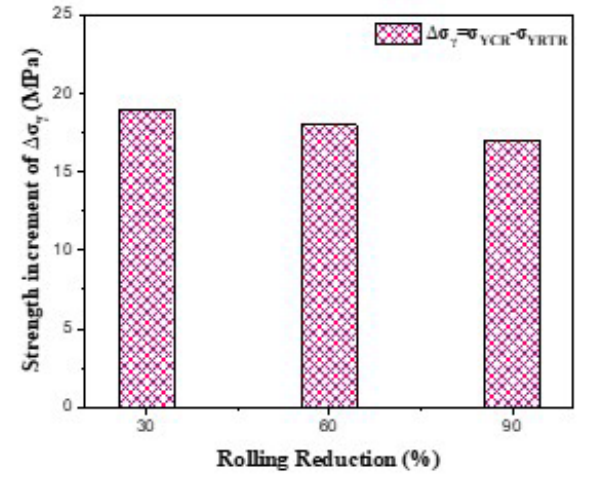

Figure 5: The YS variation Strengthening increment (Δσ_Y).

As further rolling reduction was performed in the second phase, it was discovered that the average particle size decreased. Comparing CR and RTR samples subjected to the same rolling reduction circumstances reveals that the former has a smaller average second particle size. That's an example of the second-stage particle size reduction possible with CR processing. Authors [25] showed that second-stage particles easily break apart during deformation. Shear stress is probably responsible for this result (Figure 6) [26]. An overview of shear stress and its function is as follows:

$$\tau = \frac{\sigma}{2} \sin 2\theta \quad (4)$$

where θ represents the angular direction between the compression and the shear stress, σ represents the flow stress, and τ represents the stress of shear.

According to study [27] the stress of flow is significantly maximum at 79 than at 295 K throughout the deformation phase. The production of higher densities of displacements at lower temperatures increases the flow stress, leading to these effects. This is because dynamic recovery is significantly hindered by the presence of low temperatures. As indicated by equation 4, a high shear stress can be generated using CR, causing particles in the second phase to undergo size reduction.

The solidification contribution of, Al (Ir, Mg) materials (σ_p) to the YS, (σ_Y) was calculated for RTR and CR -processed samples using equations 2 and equation 3.

The strong increment of precipitation $(\Delta\sigma_P = \sigma_{PCR} - \sigma_{PRTR})$ is shown in figure 7 to be responsible for the YS rises during the transition from cryo rolling to RTR operations. In a comparison between a sample taken at room temperature and one taken at CR with the same rolling reduction, the stronger contribution of second-stage components to the YS is most evident. This is because in the second stage of the CR specimens, the mean particle size is less than in the RTR specimens.

The YS (σ_Y), (σ_{dis}) is increased by the dislocation reinforcing contribution [28].

$$\sigma_{dis} = \alpha M G b \sqrt{\rho} \quad (5)$$

For a face-centered cubic alloy, ρ = 0.2 is a stable value where α is defined as the dislocation density. In this investigation, EBSD was used to calculate the dislocation densities. The geometrically needed dislocation (GND) density in the RTR and CR specimens was calculated using equation 6 [29].

$$\rho^{GND} = 2\theta/\mu_b \quad (6)$$

Specifically, $\left(KAM_{ave} = \exp\left[\frac{1}{N}\sum_1^i \ln KAM_{L,i}\right]\right), KAM_{ave}$, where i is the mean value of specific localised misorientation at those points.

Typical values of Kernel Average Misorientation (KAM) look like this: In this notation, KAM_{ave} stands for the evaluated region's average KAM value, KAM_{Li} represents the KAM value at position I in the evaluated region, μ denotes for the actual step size recorded and N represents the quantity of points in the evaluated region. Figure 8 displays the GND

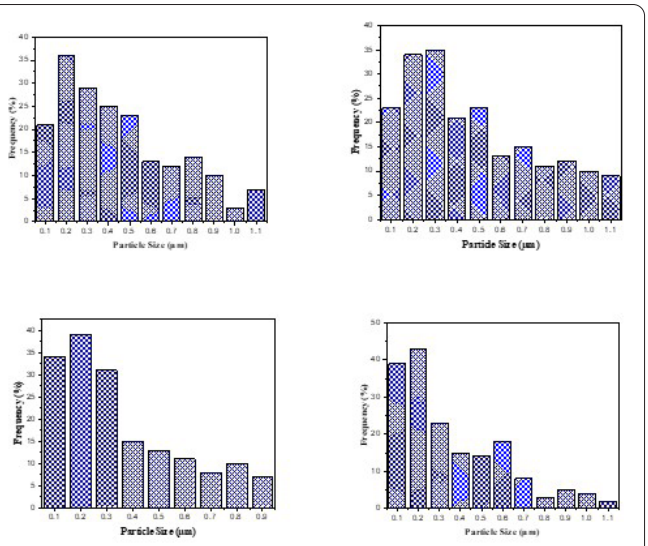

Figure 6: Particle-size distribution of the ST specimen at **(a)** CR 30, **(b)** RTR 30, **(c)** CR 90, and **(d)** RTR 90 conditions.

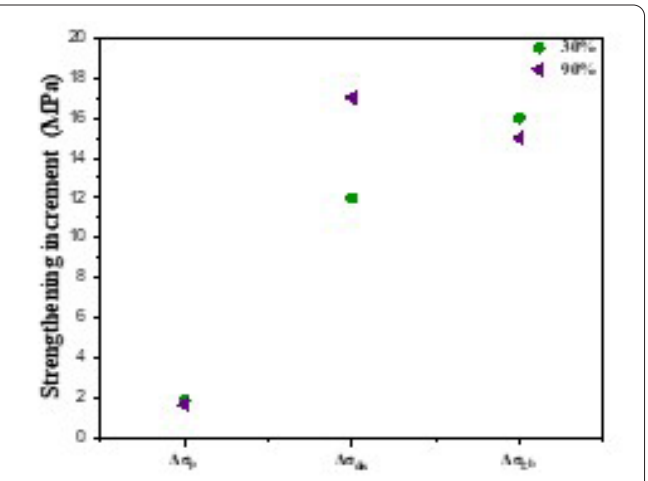

Figure 7: The strengthening increments to the YS.

dislocation densities of rolled samples at ambient temperature and samples that were CR with different levels of reduction.

As rolling reduction was raised, the dislocation density increased both at cryogenic temperatures and ambient temperature. Dislocation density is not affected by rolling reduction but is higher in cryogenically rolled samples than in RTR specimens of the same rolling reduction. This is because dislocations accumulated more, and new dislocations were created since dynamic recovery was slowed down by the CR process [30]. RTR and CR specimens have different dislocation strengthening involvement σ_{dis} to the YS σ_Y ratios, which may be calculated using equation 5 and 6. The dislocation strengthening involvement (σ_{dis} to the YSσY) of the CR sample at 30% and 90 % rolling reduction was shown in figure 8 to be 9 and 12 MPa greater, respectively, than that of the RTR specimen. This is because CR specimens have a high displacement concentration.

Grain barriers with considerable misorientation (≥16°) act as active displacement blocks during plastic deformation, limiting the transfer of moveable displacement from one crystal

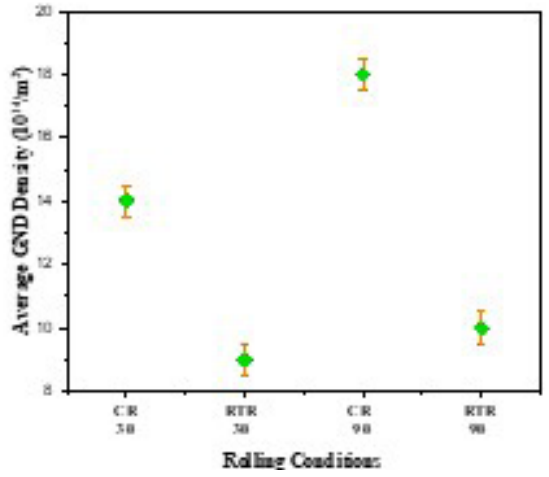

Figure 8: Different rolling conditions and dislocation densities.

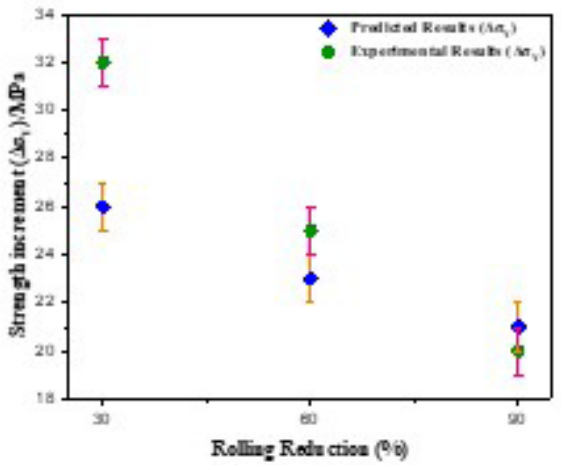

Figure 9: Predicted and experimental findings for the strengthening increment $(\Delta\sigma_Y)$ are compared and contrasted with regard to CR (σ_{YCR}) and RTR (σ_{YRTR}).

to its neighbor and raising the UTS and YS in metals. Because there are many more grain boundaries per unit area in very fine grains, the effect of this reinforcing is amplified. Increases in refined grain input are represented by the following relationship (σ_{gb}) = YS(σ_Y).

$$\sigma_{gb} = kd^{-1/2} \quad (7)$$

Hall-Petch constant (k) and mean grain size (d) are the two variables. The standard value of k for AA 5052 is $0.076 MPam^{1/2}$. Grain improvement σ_{gb} to the YSσ_Y is realizable for both the RTR and CR specimens, as displayed by equation 7 . Figure 6 shows that the grain enhancement σ_{gb} to the YS σ_Y in the cryo sample was 9 and 6 MPa bigger than in the RTR sample at 30% and90 % rolling reduction, respectively. Figure 9 compares the theoretical and experimental values of the difference between σ_{YCR} and σ_{YRTR} which represents the strengthening increment $(\Delta\sigma_Y)$. Good agreement was established between the predicted and observed outcomes. These findings imply that YS in AA5052 is more dependent on grain refinement and dislocation strengthening than on precipitation strengthening.

Conclusions

This study examined the impact of RTR and CR processing on the mechanical properties of AA5052. The most important results are summarized below.

- Dislocation density in AA5052 increased dramatically, whereas mean grain size and second-stage components decreased during RTR and CR processing. The CR specimen has the same amount of rolling reduction as the RTR and CR specimens, but its sub-grain size and dislocation density are substantially smaller.
- When comparing CR processing to RTR processing, AA5052 benefits substantially in terms of YS, maximum TS, and EL. The enhanced strength is mostly the result of dislocation and grain refining strengthening.

Acknowledgements

None.

Conflict of Interest

None.

References

1. Kumar DD, Balamurugan A, Suresh KC, Kumar RS, Jayanthi N, et al. 2023. Study of microstructure and wear resistance of AA5052/B_4C nanocomposites as a function of volume fraction reinforcement to particle size ratio by ANN. *J Chem* 2023: 1-12. https://doi.org/10.1155/2023/2554098
2. Srinivasan R, Karunakaran S, Hariprabhu M, Arunbharathi R, Suresh S, et al. 2023. Investigation on the mechanical properties of powder metallurgy-manufactured AA7178/$ZrSiO_4$ nanocomposites. *Adv Mater Sci Eng* 2023: 1-11. https://doi.org/10.1155/2023/3085478
3. Bothiraj T, Boopathi K, Kalaiselvan K, Benham A, Mayakannan S. 2022. Experimental investigations on mechanical and wear behavior of waste marble dust and coconut fiber reinforced hybrid bio composites. *Mater Today Proc* 68: 2239-2242. https://doi.org/10.1016/j.matpr.2022.08.441
4. Wu HY, Yang LJ, Du LX, Gao XH. 2020. Effect of annealing process on microstructure and mechanical properties of cryorolled 6061 aluminum alloy. *Trans Mater Heat Trt* 41(5): 72-78. https://doi.org/10.13289/j.issn.1009-6264.2018-0119
5. Zha J, Zhao Y, Qiao Y, Zou H, Hua Z, et al. 2023. Effect of rolling process and aging on the microstructure and properties of Cu-1.0 Cr-0.1 Zr alloy. *Materials* 16(4): 1592. https://doi.org/10.3390/ma16041592
6. Shi J, Hou L, Zuo J, Zhuang L, Zhang J. 2017. Cryogenic rolling-enhanced mechanical properties and microstructural evolution of 5052 Al-Mg alloy. *Mater Sci Eng* 701: 274-284. https://doi.org/10.1016/j.msea.2017.06.087
7. Liu H, Wang Y, Li B, Ma X, Wu R, et al. 2019. Effect of cryogenic rolling process on microstructure and mechanical properties of Mg-14Li-1Al alloy. *Mater Charact* 157: 109903. https://doi.org/10.1016/j.matchar.2019.109903
8. Yang QY, Zhou YL, Tan YB, Xiang S, Ma M, et al. 2021. Effects of microstructure, texture evolution and strengthening mechanisms on mechanical properties of 3003 aluminum alloy during cryogenic rolling. *J Alloys Compd* 884: 161135. https://doi.org/10.1016/j.jallcom.2021.161135
9. Li R, Xiao Z, Li Z, Meng X, Wang X. 2023. Work hardening behavior and microstructure evolution of a Cu-Ti-Cr-Mg alloy during room temperature and cryogenic rolling. *Materials* 16(1): 424. https://doi.org/10.3390/ma16010424

10. Li HP. 2018. Effect of deformation temperatures on microstructure and mechanical properties of 316LN austenitic stainless steel. *Trans Mater Heat Trt* 39(3): 50-57.
11. Liao W, Qiang H, Song W, Hu Y, Zhang C. 2023. Effect and mechanism of room temperature rolling, cryogenic rolling and heat treatment on mechanical properties and electrical conductivity of Cu-Ni-Si alloy with continuous directional solidification. *J Alloys Compd* 949: 169748. https://doi.org/10.1016/j.jallcom.2023.169748
12. Arunprasath K, Murugan G, Selvakumar P, Thirumavalavan S, Mareeswaran S, et al. 2023. Study of mechanical characteristics and strengthening mechanism of AA5154 during cryogenic rolling. *Mater Today Proc* 2023. https://doi.org/10.1016/j.matpr.2023.02.330
13. Satishkumar P, Mahesh G, Meenakshi R, Vijayan SN. 2021. Tribological characteristics of powder metallurgy processed Cu-WC/SiC metal matrix composites. *Mater Today Proc* 37: 459-465.
14. Elsheikh AH, Shanmugan S, Muthuramalingam T, Thakur AK, Essa FA, et al. 2022. A comprehensive review on residual stresses in turning. *Adv Manuf* 1-26. https://doi.org/10.1007/s40436-021-00371-0
15. Satishkumar P, Rakesh AI, Meenakshi R, Murthi CS. 2021. Characterization, mechanical and wear properties of Al6061/Sicp/fly ashp composites by stir casting technique. *Mater Today Proc* 37: 2687-2694. https://doi.org/10.1016/j.matpr.2020.08.530
16. Satyanarayana G, Narayana KL, Rao BN. 2021. Incorporation of Taguchi approach with CFD simulations on laser welding of spacer grid fuel rod assembly. *Mater Sci Eng* 269: 115182. https://doi.org/10.1016/j.mseb.2021.115182
17. Satishkumar P, Krishnan GG, Seenivasan S, Rajarathnam P. 2023. A study on tribological evaluation of hybrid aluminium metal matrix for thermal application. *Mater Today Proc* 81: 1097-1104. https://doi.org/10.1016/j.matpr.2021.04.389
18. Dharmaiah G, Sridhar W, Balamurugan KS, Chandra Kala K. 2022. Hall and ion slip impact on magneto-titanium alloy nanoliquid with diffusion thermo and radiation absorption. *Int J Ambient Energy* 43(1): 3507-3517. https://doi.org/10.1080/01430750.2020.1831597
19. Abushanab WS, Moustafa EB, Harish M, Shanmugan S, Elsheikh AH. 2022. Experimental investigation on surface characteristics of Ti6Al4V alloy during abrasive water jet machining process. *Alex Eng J* 61(10): 7529-7539. https://doi.org/10.1016/j.aej.2022.01.004
20. Won JW, Choi SW, Hong JK, Suh BC, Lee JH, et al. 2020. Microstructure and strength–ductility balance of pure titanium processed by cryogenic rolling at various rolling reductions. *Mater Sci Eng* 798: 140328. https://doi.org/10.1016/j.msea.2020.140328
21. Wu W, Guo L, Guo B, Liu Y, Song M. 2019. Altered microstructural evolution and mechanical properties of CoCrFeNiMo0. 15 high-entropy alloy by cryogenic rolling. *Mater Sci Eng* 759: 574-582. https://doi.org/10.1016/j.msea.2019.05.078
22. Arunprasath K, Murugan G, Selvakumar P, Thirumavalavan S, Mareeswaran S, et al. 2023. Study of mechanical characteristics and strengthening mechanism of AA5154 during cryogenic rolling. *Mater Today Proc* 2023. https://doi.org/10.1016/j.matpr.2023.02.330
23. Moradpour M, Khodabakhshi F, Eskandari H. 2019. Dynamic strain aging behavior of an ultra-fine grained Al-Mg alloy (AA5052) processed via classical constrained groove pressing. *J Mater Res Technol* 8(1): 630-643. https://doi.org/10.1016/j.jmrt.2018.04.016
24. Wei H, Chen Y, Li Z, Shan Q, Yu W, et al. 2021. Microstructure evolution and dislocation strengthening mechanism of Cu–Ni–Co–Si alloy. *Mater Sci Eng* 826: 142023. https://doi.org/10.1016/j.msea.2021.142023
25. Kumar N, Gautam G, Gautam RK, Mohan A, Mohan S. 2017. A study on mechanical properties and strengthening mechanisms of AA5052/ZrB2 *in situ* composites. *J Eng Mater Technol* 139(1): 011002. https://doi.org/10.1115/1.4034692
26. Ji Q, Zhang S, Wu R, Jin S, Zhang J, et al. 2022. High strength BCC magnesium-Lithium alloy processed by cryogenic rolling and room temperature rolling and its strengthening mechanisms. *Mater Charact* 187: 111869. https://doi.org/10.1016/j.matchar.2022.111869
27. Gao Y, Li H, Zhao D, Wang M, Fan X. 2023. Cryogenic friction behavior of aluminum alloys sheets under dry contact condition. *Tribol Int* 180: 108227. https://doi.org/10.1016/j.triboint.2023.108227
28. Mohebbi MS, Akbarzadeh A. 2018. Constitutive equation and FEM analysis of incremental cryo-rolling of UFG AA 1050 and AA 5052. *J Mater Process Technol* 255: 35-46. https://doi.org/10.1016/j.jmatprotec.2017.11.061
29. Zuiko IS, Mironov S, Kaibyshev R. 2019. Microstructural evolution and strengthening mechanisms operating during cryogenic rolling of solutionized Al-Cu-Mg alloy. *Mater Sci Eng* 745: 82-89. https://doi.org/10.1016/j.msea.2018.12.103
30. Moradpour M, Khodabakhshi F, Eskandari H. 2018. Microstructure–mechanical property relationship in an Al–Mg alloy processed by constrained groove pressing-cross route. *Mater Sci Technol* 34(8): 1003-1017. https://doi.org/10.1080/02670836.2017.1416906